



HAL
open science

Molecular features of hepatosplenic T-cell lymphoma unravels potential novel therapeutic targets.

Marion Travert, Yenlin Huang, Laurence de Leval, Nadine Martin-Garcia, Marie-Helene Delfau-Larue, Françoise Berger, Jacques Bosq, Josette Brière, Jean Soulier, Elizabeth Macintyre, et al.

► **To cite this version:**

Marion Travert, Yenlin Huang, Laurence de Leval, Nadine Martin-Garcia, Marie-Helene Delfau-Larue, et al.. Molecular features of hepatosplenic T-cell lymphoma unravels potential novel therapeutic targets.. Blood, 2012, 119 (24), pp.5795-806. 10.1182/blood-2011-12-396150 . inserm-00730464

HAL Id: inserm-00730464

<https://inserm.hal.science/inserm-00730464v1>

Submitted on 1 Oct 2012

HAL is a multi-disciplinary open access archive for the deposit and dissemination of scientific research documents, whether they are published or not. The documents may come from teaching and research institutions in France or abroad, or from public or private research centers.

L'archive ouverte pluridisciplinaire **HAL**, est destinée au dépôt et à la diffusion de documents scientifiques de niveau recherche, publiés ou non, émanant des établissements d'enseignement et de recherche français ou étrangers, des laboratoires publics ou privés.

MOLECULAR FEATURES OF HEPATOSPLENIC T-CELL LYMPHOMA UNRAVELS POTENTIAL NOVEL THERAPEUTIC TARGETS

Marion Travert^{1,2,3}, Yenlin Huang^{1,2,4}, Laurence de Leval⁵, Nadine Martin-Garcia^{1,2,3}, MH Delfau-Larue^{1,2,6}, Françoise Berger⁷, Jacques Bosq⁸, Josette Brière⁹, Jean Soulier¹⁰, Elizabeth MacIntyre¹¹, Teresa Marafioti^{2,12}, Aurélien de Reyniès^{13*}, Philippe Gaulard^{1,2,3*}

(1) Inserm U955, Créteil, 94000, France; (2) Université Paris-Est, Créteil, 94000, France; (3) Département de Pathologie, AP-HP, Groupe Henri-Mondor Albert-Chenevier, Créteil, France; (4) Department of Anatomic Pathology, Chang Gung Memorial Hospital, Gueishan, 33305, Taiwan. (5) Institute of Pathology, CHUV, University of Lausanne, Switzerland; (6) Service d'Immunologie Biologique, AP-HP, Créteil, France, (7) Département de Pathologie, Hôpital Lyon-Sud, Pierre-Benite, France ; (8) Department of Medical Biology and Pathology, Institut Gustave Roussy, Villejuif, France; (9) INSERM U728 et Service de Pathologie, Hôpital Saint Louis, Paris, France; (10) INSERM U976, Hôpital Saint Louis, Paris, France; (11) Hématologie, AP-HP Necker-Enfants-Malades and Université Paris Descartes, Paris, France; (12) Department of Histopathology, University College Hospital London, London, United Kingdom ; (13) Ligue Nationale Contre le Cancer, Paris, France.

*P.G. and A.d.R. contributed equally to this work

RUNNING TITLE: Molecular Signature of Hepatosplenic T-cell Lymphoma

WORD COUNTS FOR TEXT: 4581

WORD COUNTS FOR ABSTRACT: 200

REFERENCE COUNT: 60

SCIENTIFIC CATEGORY: lymphoid neoplasia

ABSTRACT

Hepatosplenic T-cell lymphoma (HSTL) is a rare entity mostly derived from $\gamma\delta$ T cells that shows a fatal outcome. Its pathogenesis remains largely unknown. HSTL samples ($7\gamma\delta$, $2\alpha\beta$) and the DERL2 HSTL-cell line were subject to combined gene expression profiling and array-based comparative genomic hybridization. Compared to other T-cell lymphomas, HSTL disclosed a distinct molecular signature irrespective of TCR cell lineage. Compared to PTCL,NOS and normal $\gamma\delta$ cells, HSTL overexpressed genes encoding NK-cell associated molecules, oncogenes (*FOS*, *VAV3*), the Sphingosine-1-phosphatase receptor 5 involved in cell trafficking and the tyrosine kinase *SYK*, whereas the tumor suppressor gene *AIM1* was among the most downexpressed. Methylation analysis of DERL2 cells demonstrated highly methylated CpG islands of *AIM1* and decitabine treatment induced significant increase in *AIM1* transcripts. Notably, Syk was demonstrated in HSTL cells with its phosphorylated form present in DERL2 cells by Western blot, and *in vitro* DERL2 cells were sensitive to a Syk inhibitor. Genomic profiles confirmed recurrent isochromosome 7q (n=6/9) without alterations at 9q22 and 6q21 containing *SYK* and *AIM1* genes, respectively. The current study identifies a distinct molecular signature for HSTL and highlights oncogenic pathways which offer rationale for exploring new therapeutic options such as Syk inhibitors and demethylating agents.

INTRODUCTION

Hepatosplenic T-cell lymphoma (HSTL), originally described as *hepatosplenic $\gamma\delta$ T cell lymphoma*, is a rare lymphoma entity with peculiar clinical presentation - hepatosplenomegaly without significant lymphadenopathy - and pathological features - intrasinusal/sinusoidal infiltration by neoplastic T cells in the bone marrow, spleen and liver¹⁻³. The disease occurs predominantly in young adults, in association with a setting of long-term immunosuppression in solid organ transplant recipients or with prolonged antigenic stimulation⁴. Cases have also been reported in children treated by azathioprine and infliximab for Crohn's disease⁵. While most HSTL are derived from the $\gamma\delta$ subset, a few similar cases with an $\alpha\beta$ phenotype have also been described^{6,7}, and the simplified designation "hepatosplenic T-cell lymphoma" was favored in the latest World Health Organization classification⁸. HSTL is associated with a recurrent isochromosome 7q and less often, trisomy 8⁹, but its pathogenesis remains largely unknown.

Despite relatively innocuous cytology, the disease is highly aggressive with an almost constant fatal outcome and a median overall survival barely exceeding one year⁴. Occasional long survivors have been reported and few patients respond to cytarabine or deoxycoformycin^{4,10}. Therapeutic strategies curative in a significant proportion of other aggressive subtypes of lymphoma, have proved to be ineffective in HSTL and efficient treatment modalities remain to be defined.

Over the past years, genome-wide molecular profiling studies have contributed significant insights to the pathobiology of several T-cell lymphoma entities¹¹⁻¹⁴ and brought informative data on the multiple molecular subgroups in PTCL, not otherwise specified (PTCL,NOS)^{15,16}. In that respect, data on HSTL are scarce^{13,17}. In the current study, we analyzed a series of HSTL samples in relation to normal $\gamma\delta$ cells, PTCL,NOS and extranodal NK/T-cell lymphoma, nasal-type (NKTCL), another entity derived from cytotoxic lymphocytes of the innate immune system. The aim of the study was to (1) characterize the molecular signature of HSTL, (2) identify potential

candidate pathways relevant to pathogenesis, and (3) search for biomarkers useful in the diagnostic purposes or in the future targeted therapies.

PATIENTS, MATERIALS AND METHODS

Patient characteristics and tumor samples

Nine HSTL patients with high quality RNA and/or DNA extracted from frozen tumor samples were selected for this study. All patients had spleen, liver and bone marrow involvement without lymphadenopathies. Three patients had been included in previous reports^{4,9}. The main clinical, phenotypic and molecular characteristics are summarized in Table 1. The tumor samples, comprised six splenic tissue samples and three cell suspensions (from spleen, bone marrow and blood), two of which were enriched in tumor cells (samples HSTL_01 and HSTL_09). All cases were reviewed by three hematopathologists (L.d.L, Y.H. and P.G.) and diagnosed according to the WHO criteria⁸. The tumor cells had a CD3+, CD2+, CD5-, TiA1+, GzmB-immunophenotype and were negative for EBV. T-cell receptor (TCR) lineage was determined by immunohistochemistry and/or flow cytometry for TCR β and TCR δ chain expression and by GC-clamp multiplex PCR for TCR γ and/or δ chain rearrangements ((PCR)- δ -DGGE procedure)¹⁸. In total, seven cases with a δ TCR1+, β F1- immunophenotype and/or a biallelic rearrangement of the TCR δ chain^{18,19}, were classified as $\gamma\delta$ HSTL and two cases with a δ TCR1-, β F1+ phenotype as $\alpha\beta$ HSTL. Four of seven investigated cases disclosed isochromosome 7q.

Twelve additional HSTL cases were selected for validations (10 formalin-fixed tissues for immunohistochemistry and 2 frozen samples for RT-PCR analyses).

The study was approved by the institutional review board “Comité de Protection des Personnes Ile de France IX”, Créteil, France CPP N°08-009 (06/05/08).

Cell lines and normal $\gamma\delta$ T cells

Eight samples of normal peripheral blood activated $\gamma\delta$ T cells (6 from Correia²⁰ and 2 from Zhang²¹) and 3 samples of normal resting $\gamma\delta$ T cells (from Correia²⁰) were used for comparison. Normal $\gamma\delta$ T cells sorted using magnetic anti-TCR $\gamma\delta$ microbeads kit (Miltenyi Biotec, Bergisch Gladbach, Germany) from 3 spleens removed for benign conditions were also obtained for qRT-PCR validation. DERL2, a $\gamma\delta$ cell line derived from HSTL²², was cultured in IMDM supplemented with 2 mM L-glutamine and 20% heat-inactivated human serum (Invitrogen, Carlsbad, CA) in the presence of recombinant human interleukin (IL)-2 (100 U/ml, Laboratoires Chiron, Amsterdam). Centrifugated pellets of DERL2 cells were fixed in ethanol to construct paraffin-embedded blocks¹⁴.

Microarray procedures

Microarray analyses, from extraction to labeling and hybridization, were performed as previously reported^{11,14}.

Gene expression analyses

HG-U133-plus-2.0 Affymetrix array data were obtained for nine HSTL and the DERL-2 cell line (Table 1) and deposited to ArrayExpress under accession number E-MTAB-638. HG-U133-plus-2.0 profiles of 42 PTCL-NOS, 23 AITL, 23 NKTCL and 3 HSTL previously reported by our group (E-TABM-783, E-TABM-702, n=40)^{11,14} and others (GSE19067, GSE6338, n=51)^{12,13} were used for analyses. Control samples (8 activated $\gamma\delta$ T-cells, 3 resting $\gamma\delta$ T-cells, 18 B-cells, 6 spleens and 9 lymph nodes) were collected by us (n=6) or from public sources (E-MEX-1601, GSE13906, GSE12195, GSE15271, GSE7307)^{20,21,23,24}. Affymetrix raw data of all samples were normalized in batch using RMA algorithm. The clustering analysis of the 50 tumor samples from our series was performed as already described¹⁴. We used moderate T-tests to identify genes

differentially expressed between two groups of samples and AUC criteria to identify discriminant genes. KEGG and Biocarta pathways (and related genes) were obtained from <ftp://ftp.genome.ad.jp/pub/kegg/pathways/hsa> and <http://www.biocarta.com>. Pathways were ranked according to the scores of three different algorithms including globaltest, SAM-GS and GSA. Methodological details are given in the Supplementary Materials and Methods (Method S1).

Array-based comparative genomic hybridization

DNAs extracted from 7 HSTL and DERL2 cell line were hybridized on Agilent Sureprint CGH array 4 x 180 k covering over 170,000 coding and non-coding human sequences. CGH array raw Cy3/Cy5 intensities were quantile normalized independently for each sample; smoothing was performed using tilingArray R package, copy number status (Gain/Loss) determination in the smoothed segments was done as previously reported¹⁴. Details are given as supplemental (Method S1).

Quantitative reverse-transcriptase PCR analysis of candidate genes

The expression level of candidate genes (*FOS*, *FOSB*, *AIM1*, *RHOB*, *ABCBI*, *VAV3*, *KIR3DS1*, *SIPR5*) identified in gene expression analysis was determined by TaqMan[®] quantitative reverse-transcriptase PCR (qRT-PCR) (Applied Biosystems, Foster City, CA) in 11 primary HSTL tumors (including the 9 cases submitted to GEP analysis), the DERL2 cell line and 3 normal splenic $\gamma\delta$ T cell samples as control. All primers and probes were purchased from Applied Biosystems and the gene expression was measured using Mastercycler[®] ep realplex^{2S} system (Eppendorf, Hamburg, Germany). Quantifications were done in duplicate and mean values and standard deviation were calculated for each transcript as previously described²⁵.

Immunohistochemical analysis of selected candidate genes

Immunohistochemistry was performed on deparaffinized tissue sections using a standard indirect avidin-biotin immunoperoxidase method. After appropriate antigen retrieval, sections were stained for FosB (Cell Signaling Technology, Danvers, MA); CD56, CD163 and GSTP1 (Novocastra-Leica, Wetzlar, Germany); β -catenin (BD Biosciences, San Diego, USA); Bcl-10 (Zymed, San Francisco, USA), ICAM-1 (Atlas Antibodies, Stockholm, Sweden), VCAM-1 and Syk (Santa Cruz Biotechnology, Santa Cruz, USA), Blimp-1 (BioLegend UK Ltd, Cambridge, UK). For granzyme H (gzm H)(4G5) a tyramide signal amplification system was applied, as previously described¹⁴. Adequate controls were included.

Methylation analysis of AIM1

Two μ g of genomic DNA were treated with bisulfite using the Epiect[®] Bisulfite Kit (Qiagen, Courtaboeuf, France) according to manufacturer's protocol. Nested bisulfite-specific PCR for the 2 CpG islands of *AIM1* was performed on DERL2 cells DNA (details, primers and PCR programs used are given in Supplemental Methods (Method S1)). PCR products were cloned in plasmid using TOPO TA cloning kit for sequencing (Invitrogen). Ten clones for each CpG islands were screened and sequenced on the ABI 3130X1 genetic analyser (Applied Biosystems).

5-Aza-2'-deoxycytidine treatment of DERL2 cells

DERL2 cells were treated with the demethylating agent 5-Aza-2'-deoxycytidine (Decitabine, Merck Chemicals, Nottingham, UK) at 10 μ M or 40 μ M for 96 hours (decitabine was added every 24 hours) alone or in combination with 500 nM histone deacetylase inhibitor trichostatin A (TSA) (Sigma Aldrich, Saint-Quentin Fallavier, France). In the combined treatment (decitabine and TSA), cells were treated with 10 μ M or 40 μ M of decitabine for 96 hours (every 24 hours) followed by 500 nM of TSA for the last 24 hours. Total RNA was extracted and qRT-PCR was

performed to evaluate the re-expression of the demethylated gene *AIM1* after decitabine treatment. In addition the number of apoptotic cells was determined by Annexin V+, 7AAD+ cells using a Cyan flow cytometer (Beckman Coulter, Villepinte, France).

Immunoblot analysis

Total cell proteins extracted from normal blood T cells [purified after CD2 magnetic beads selection and activated or not by CD3 (1µg/ml), CD28 (1µg/ml) and IL2 (100U/ml)], overnight serum deprived DERL2 cells with or without CD3, CD28 and IL2 activation and overnight serum deprived SUDHL4 cells with or without BCR stimulation (anti-Fab'2, 4µg/ml) were analyzed for the expression of Syk, phospho-Syk (Tyr525/526)(C87C1) (Cell Signaling technology) and β-actin (Sigma Aldrich). Immunoblotting was done as previously described²⁵.

Apoptosis assay with a Syk inhibitor

Normal activated γδ T cells were obtained as previously described²⁶, DERL2 cells were plated at 1,000,000 cells per well. They were incubated for 48 hours in the absence or presence of Syk inhibitor II (Merck Chemicals) at 2 different concentrations (40 and 60 µM). The number of apoptotic cells was determined by Annexin V+, 7AAD+ cells. For the normal activated γδ T cells, TCRVγ9 apoptotic cells were determined by measuring the percentage of TCRVγ9+ 7AAD+ cells.

RESULTS

1 - HSTL as a molecularly distinct entity irrespective of TCR γδ or αβ lineage

Unsupervised consensus clustering of the expression profiles of 9 HSTL tumors and 41 additional T-cell lymphoma samples including PTCL,NOS, angioimmunoblastic T-cell lymphoma (AITL) and NKTCL demonstrated a clear separation between HSTL and other T-cell

lymphomas entities. The HSTL cluster comprised two subgroups consisting of HSTL tissue samples and HSTL cells (sorted cells and cell line) (Figure 1). Interestingly, $\alpha\beta$ and $\gamma\delta$ HSTL clustered together. One non-hepatosplenic $\gamma\delta$ T-cell lymphoma case (PTCL_20) with nodal presentation clustered within the NKTCL branch.

On supervised analysis, $\alpha\beta$ and $\gamma\delta$ HSTL appeared to have a highly similar gene signature. As illustrated in [supplemental figure S1](#), a similar level of transcripts of NK cell-associated molecules including killer immunoglobulin-like receptors (KIRs) were found in HSTL, irrespective of $\alpha\beta$ or $\gamma\delta$ lineage. Besides the genes coding for the $\gamma\delta$ and $\alpha\beta$ TCR which, as expected, were the most differentially expressed between both groups, only a small proportion of genes appeared overexpressed in $\gamma\delta$ HSTL (*LCK*, *SYT11*, *BCL2L11*, *KLRC1*...) or downexpressed (*CRI*, *TMPRSS3*, *ITGA9*...) compared to $\alpha\beta$ HSTL (Supplemental table S1). Comparison of HSTL gene expression profiles with that of either PTCL,NOS or NKTCL revealed similar proportions of differentially expressed genes (H1 Proportion, see Method S1) of 37% and 39% respectively), however in unsupervised clustering analysis, HSTL profiles appeared to be closer to that of NKTCL, another extranodal entity derived from cytotoxic cells, than that of PTCL,NOS and AITL.

Compared to both PTCL, NOS and NKTCL, several T-cell associated transcripts encoding the $\gamma\delta$ T-cell receptor (TCR) subunit were among the top genes overexpressed in HSTL. Two of the interesting genes found to be upregulated in HSTL were *SIPR5*, a gene known to be involved in the homing of NK cells into the spleen²⁷ and *ABCB1* encoding for the p-glycoprotein multidrug transporter (*MDR1*). These findings were confirmed by qRT-PCR that demonstrated high *SIPR5* and *ABCB1* transcripts in HSTL compared to PTCL,NOS and NKTCL (Figure 2). Genes encoding KIRs and other NK cell-associated molecules (*NCAMI*, *CD244*) were specifically overexpressed compared to PTCL, NOS (Tables 2 and 3).

AIM1, reported as a tumor suppressor gene ²⁸, was underexpressed in HSTL compared both to PTCL,NOS and NKTCL. The genes underexpressed in HSTL compared to PTCL,NOS included genes encoding T_{FH}-associated molecules (*CXCL13*, *ICOS*, *CD200*, *CXCR5*), others involved in immunomodulation (*IDO1*, *IL4I1*) as well as CD5, a T-cell surface antigen known to be absent in HSTL cells.

2 – Candidate genes relevant to HSTL pathogenesis

To search for candidate genes relevant to the pathogenesis of HSTL, we compared HSTL signature to that of normal $\gamma\delta$ T cells. A selection of significantly overexpressed and underexpressed genes distinguishing HSTL from normal activated or resting $\gamma\delta$ T cells is summarized in Table 4 (p<0.01). Among the most overexpressed genes in HSTL were those related to NK-cell associated molecules such as *KIRs*, *KLR*, *CD244* and *NCAM1*. The other overexpressed genes were related to oncogenes (*FOS*, *VAV3*, *MAF* and *BRAF*), cell adhesion (*VCAM1*, *CD11d*, *ICAM1*), tyrosine kinases (*SYK*), signal transduction (*SPRY2*, *RHOB*, *MAP4K3*, *SPRY1*), the sonic hedgehog pathway (*GLI3*, *PRKAR2B*, *PRKACB* and *PRKARIA*), the WNT pathway (*FRZB*, *TCF7L2*, *BAMBI*, *TLE1*, *CTNNB1*, *APC* and *FZD5*) and *S1PR5*. Interestingly, many of these genes appeared to be also overexpressed in HSTL sorted cells compared to normal activated or resting cells $\gamma\delta$ T cells (supplemental Table S1). This was the case for genes encoding *FOS*, *VAV3*, *RHOB*, *S1PR5* and NK-cell associated molecules indicating that their overexpression could be attributed to the neoplastic cells. These findings were confirmed by qRT-PCR analysis (Figure 2) demonstrating overexpression of *FOS*, *RHOB*, *VAV3*, *S1PR5* and *KIR3DS1* mRNAs in HSTL sorted cells, and to a lesser extent in HSTL tissues, in comparison with normal $\gamma\delta$ T cells. Furthermore, another oncogene *FOSB* (belonging to the AP1 family) was overexpressed in HSTL cells compared to activated $\gamma\delta$ T cells. This finding was corroborated by qRT-PCR analysis (Figure 2D) and by immunohistochemistry evidencing the

presence of FosB-positive cells coexpressing CD2 or TIA1 in HSTL (Figure 3A). In addition, membrane CD56 (9/17) and cytoplasmic Syk (8/9) were demonstrated in the neoplastic cells infiltrating the sinuses in the spleen or bone marrow (Figure 3C and D).

Genes associated with cytotoxicity (*Granulysin*, *Granzyme H*, *Granzyme K*, *Granzyme B*), cytokines (*LTA*, *TNF*, *IFNG*), the tumor suppressor *AIM1* and *CD5* were among genes those significantly underexpressed in HSTL compared to normal cell counterpart. Absence of expression of cytotoxic molecules such as Granzyme B (Table 1) and Granzyme H was shown by immunostaining (Figure 3H) whereas the dramatic reduction of *AIM1* transcripts was demonstrated by qRT-PCR in both HSTL tissues and sorted cells compared to normal $\gamma\delta$ cells (Figure 5A).

3 – Biomarkers discriminating HSTL from other lymphomas and normal controls

Expression of several genes in the molecular signature of HSTL appeared most likely to be attributed to the normal spleen signature. This is the case of ICAM-1, VCAM-1 and CD163 gene products, whose expression was shown by immunohistochemistry to be restricted to non neoplastic cells, that is, endothelial cells (VCAM1, ICAM1) and macrophages (CD163). To build a biomarker list differentiating HSTL from other T-cell lymphoma entities and eliminating the observed microenvironmental signature, supervised tests (see Method S1 for details) were performed between HSTL and other lymphomas (i.e. AITL, PTCL,NOS and NKTCL), HSTL and control samples (i.e. normal lymph nodes, spleen, $\gamma\delta$ T cells, B cells) as well as between HSTL obtained from tissues and cell suspensions. This yielded a list of 54 genes distinguishing HSTL from other lymphomas entities and normal controls (Supplemental Figure S2 and tables S2, S3 and S4). Among these genes were those encoding KIR molecules (*KIR3DS1*), *CD244*, *DTNBP1* and *SIPR5*. The application of this list of biomarkers to an independent series of

lymphoma samples (including 4 HSTL, 15 AITL and 11 PTCL,NOS) using a different platform¹⁷ allowed discrimination of HSTL from other PTCLs (supplemental Figure S3).

4 – Relevant pathways and genes potentially involved in HSTL resistance to therapy

Pathways analyses showed significant enrichment of a number of pathways which are involved in cancer development or can be the target of innovative treatments, such as VEGF, MAP kinase, JAK-STAT, mTOR, Notch signaling pathways, cytokine-cytokine receptor interaction, cell adhesion (Table 6 and supplemental table S5). The Wnt signature was found deregulated but activation of the pathway was not supported by immunohistochemistry since the expression of β -catenin was restricted to endothelial cells. Consistent with previous findings¹⁷, pathways related to NK-cell mediated cytotoxicity were among the most differentially expressed compared to other T-cell lymphoma entities and normal $\gamma\delta$ T cells (Figure 4A). Furthermore, as illustrated in figure 4B, many genes in the TCR signaling pathway (*VAV3*, *BCL10*), and linked to the AP1 pathway (*FOS*) were enriched in HSTL compared to PTCL,NOS and NKTCL. These finding were supported by the high levels of *VAV3*, *FOS*, *FOSB* transcripts demonstrated by qRT-PCR, and by immunohistochemical detection of Bcl-10 in the neoplastic cells of all investigated HSTL (5/5) (Figure 3D). Significant enrichment of genes in the pathways of Sprouty regulation of tyrosine kinase and the Sonic Hedgehog signaling [such as genes for the composition of cAMP-dependent kinase (PKA)(*PRKAR2B*, *PRKARIA* and *PRKACB*), the transcription factor Ci (*GLI3*), the receptor patched (*PTCH1*) and *GSK3B*] were found in HSTL (Figure 4). Interestingly, several genes in the multidrug resistance signalling pathways (*ABCB1*, *GSTP1*) were enriched in HSTL (Figure 4E) compared to PTCL, NOS and NKTCL as well as *PRDM1*, another gene reported to be associated to resistance to therapy in PTCLs²⁹. High levels of *ABCB1* transcripts were confirmed by qRT-PCR (Figure 2B) and expression of *GSTP1* and Blimp-1 was

demonstrated by immunohistochemistry in HSTL cells of all evaluated cases, as well as in DERL2 cells (Figures 3). As illustrated in figure 4F, HSTL were closer to activated $\gamma\delta$ T cells than resting $\gamma\delta$ T cells with respect to the expression of cell cycle-related genes.

5 – Isochromosome 7 q is the main recurrent genomic aberration in HSTL

The aCGH findings confirmed recurrent isochromosome 7q in 4 of the seven tested cases (60%), with only few other alterations comprising trisomy 8 as previously reported⁹, loss of 10p arm and more focal alterations (-14q,+15q, -18q -21q, -22q) in 2 to 6 cases (30-85%)(Supplemental figure S4). In order to determine whether iso7q impacts on the molecular signature, we analysed the mean expression of genes located on the 7p and 7q arms for each sample (Supplemental figure S5). This analysis clearly showed overexpression of 7q and down expression of 7p genes in all cases with iso7q aberration as well as in 2 additional cases (HSTL_08, HSTL_09) for which the iso7q status was unknown (absence of aCGHa and FISH data), one of which could be subsequently demonstrated as iso7q by FISH (HSTL_09). To identify potential candidate genes involved in iso7q, we further compared the expression level of iso7q+ HSTL cases to normal controls (i.e. activated $\gamma\delta$ T cells). Among the most repressed genes on 7p arm were *CYCS*, *IKZF1* associated to regulation of apoptosis and *HUS1*, *CBX3* involved in DNA repair, while the most overexpressed genes on 7q arm included the putative oncogene *PTPN12* (Supplemental Table S1). Moreover, pathway analysis comparing iso7q+ HSTL to activated or resting $\gamma\delta$ T cells showed a significant enrichment of apoptosis-related pathways (Supplemental Table S5).

6 – *AIM1* is methylated in HSTL

AIM1 (absent in melanoma 1), initially described as a tumor suppressor gene deleted in melanoma, was subsequently found to be deregulated in NKTCL^{28,30}. Here we show significant downexpression of *AIM1* mRNA in HSTL and DERL2 cells. Low levels of *AIM1* mRNAs were confirmed by qRT-PCR in HSTL primary tumors and in DERL2 cells compared to normal $\gamma\delta$ T

cells (Figure 5A). We further searched for genetic alterations underlying *AIM1* downregulation. In the absence of genomic imbalance in *AIM1* locus at 6q21 in aCGH data, we asked whether *AIM1* downregulation in HSTL could be the result of methylation as already reported in other hematologic malignancies such as myeloma and NKTCL^{30,31}. The promoter methylation status of *AIM1* was analysed in the HSTL-derived cell line, DERL-2. Sequencing of *AIM1* on bisulfite-treated DNA revealed methylation in both CpG islands (Figure 5B). Furthermore, the treatment of DERL2 cells with *AIM1* methylated promoter with the DNA demethylating agent decitabine with or without TSA resulted in a 2-3 fold increase in *AIM1* mRNA level compared to untreated cells, supporting that *AIM1* downexpression in HSTL could be reversed by demethylation (Figure 5C). Interestingly, the number of DERL2 apoptotic cells was increased after decitabine treatment (Figure 5D).

7 – Syk as a candidate target for pharmacologic inhibition in HSTL

Whereas normal mature T lymphocytes lack Syk expression, Syk protein has been recently reported to be aberrantly expressed in many PTCLs³². GEP analysis revealed overexpression of *SYK* mRNA in HTSL tissues, in HSTL sorted cells and in the DERL2 cell line compared to normal $\gamma\delta$ T cells (Figure 6A). We further demonstrated Syk expression by neoplastic HSTL cells and DERL2 cells, by immunohistochemistry and western blot (Figures 3B, 6B and 6C). Because expression of Syk does not provide information on its activity, we analyzed the phosphorylation status of Syk in DERL2 cells using a phospho-specific anti-Syk (Tyr525/526) antibody. Syk was constitutively activated in DERL2 cells (Figure 6C). The mechanism leading to Syk activation is unclear as neither *SYK* amplification nor ITK-SYK fusion was detected by FISH analysis in DERL2 cells (data not shown). To determine whether Syk could contribute to the growth and survival of neoplastic HSTL cells, a chemical anti-Syk agent was used to inhibit Syk activity in

DERL2 cells. Syk inhibition induced a significant increase in apoptosis in a dose-dependent manner [in DERL2 cell line as compared to normal activated \$\gamma\delta\$ T cells](#) (Figure 6D).

DISCUSSION

HSTL is a rare and distinct PTCL entity of unknown pathogenesis. The disease is characterized by a peculiar distribution of the neoplastic cells, most often of $\gamma\delta$ T-cell derivation, within sinuses of the spleen, the liver and bone marrow and by the clinical fatal outcome. Previous scarce reports showed that HSTL has a distinct gene signature^{13,17}. Taking advantage of the exceptional availability of samples enriched in tumor cells, we show by consensus clustering that HSTL expression profiles clustered in a single branch independently of the spleen, marrow or blood origin of the diagnostic samples indicating that this signature is independent of the microenvironment. The distinct signature was further confirmed when a gene list was constructed by eliminating the signature of the normal spleen and lymph nodes. HSTL was initially reported as of $\gamma\delta$ T-cell derivation but similar cases with a $\alpha\beta$ phenotype have been later reported. In the present study, we show that two cases of HSTL with a $\alpha\beta$ phenotype had a gene signature and also a genomic profile which were highly similar to the classical $\gamma\delta$ HSTL variant providing strong molecular arguments for grouping $\gamma\delta$ and $\alpha\beta$ HSTL as a single entity as proposed in the current WHO classification⁸. The similar $\alpha\beta$ and $\gamma\delta$ HSTL molecular signature was largely contributed by [genes implicated in cytotoxic T- and NK-cell function and development](#), suggesting that both $\alpha\beta$ and $\gamma\delta$ variants are derived from subsets of cells of the innate immune system^{8,33,34}. [Indeed, a subset of \$\alpha\beta\$ T cells, referred as NK/T cells, share characteristics with NK cells and \$\gamma\delta\$ T cells including expression of CD161 \(KLRB1\), CD16, CD56, KIRs molecules and participate with NK cells and \$\gamma\delta\$ T cells in the innate immune system³⁵](#). $\gamma\delta$ T cells can accumulate in immunosuppressed patients and in the setting of chronic antigen stimulation. Expansion of $\gamma\delta$

T cells has especially been reported in patients with kidney transplantation, systemic lupus, Hodgkin lymphoma or malaria⁴ and more recently also after treatment with anti-TNF agents³⁶.

The elective distribution of the neoplastic cells within the sinuses and sinusoids of the bone marrow, spleen and liver is remarkable and accounts for the peculiar clinical presentation of HSTL with hepatosplenomegaly and cytopenia but without lymphadenopathy and leukemic pictures. Interestingly, one of the gene with the highest fold change of expression compared to PTCL,NOS and NKTCL and to a lesser extend in normal $\gamma\delta$ T cells was Sphingosine-1-phosphatase receptor 5 (*S1PR5*). *S1PR5* encodes a member of the family of S1P receptors known to be involved in T- and B-cell exit from lymphoid organs³⁷. *S1PR5* is preferentially expressed by mature CD56^{dim} human NK cells³⁸ and is involved in NK cell trafficking in steady-state and inflammatory situations. It has been reported that *S1PR5*-deficient mice have defective homing of NK cells to blood and spleen^{27,38}. Although the role of *S1PR5* in $\gamma\delta$ T cells is uncharacterized, the high level of *S1PR5* mRNA in HSTL might explain the peculiar distribution and accumulation of neoplastic $\gamma\delta$ cells in the spleen and bone marrow, preventing tumor cells from exiting sinusoids. Whether cell-cell interaction involving the cell adhesion molecule LFA1 (CD11a) expressed by HSTL cells and VCAM1 expressed by splenic sinusoidal cells could also play a role in the clinicopathologic picture of the disease remains to be determined.

Although our GEP findings were based on the comparison with normal blood $\gamma\delta$ T cells and not with splenic $\gamma\delta$ T cells, the down or overexpression of selected genes compared to normal splenic $\gamma\delta$ T cells was validated by qRT-PCR. From the present study it appears that several candidate genes involved in distinct pathways (i.e. TCR signalling, cell cycle, sonic hedgehog, sprouty regulation of tyrosine kinase pathways and multi-drug resistance) could potentially be associated with the pathophysiology of HSTL. One of the genes we found overexpressed in HSTL is *MDR-1*, whose expression was significant for this lymphoma upon comparison with normal $\gamma\delta$ T cells, PTCL,NOS and NKTCL. The P-Glycoprotein (P-gp), encoded by *MDR-1*, is

able to export drugs out of the cytoplasm, thus reducing the intracellular accumulation of cytotoxic drugs. P-gp has been reported to be overexpressed and associated with poor outcome in various hematological malignancies including NKTCL and in DLBCL^{39,40,41}. Interestingly, sensitivity to aracytine is not influenced by P-gp overexpression in multidrug resistant cell lines⁴². Although HSTL is reported as a fatal disease, recent reports have described long survivors after cytarabine-based chemotherapy⁴. The present findings might provide a rationale for the use of cytarabine containing regimen in HSTL. In addition to P-gp expression we demonstrated that Glutathione-S-transferases (GSTs), another molecule involved with resistance to alkylating agents and anthracyclines⁴³ was also expressed by the neoplastic HSTL cells (as shown by immunohistochemistry). One could hypothesise that the combination of P-gp and GST-pi expression might contribute to the resistance to anthracyclin-based chemotherapy regimen of HSTL and its poor outcome. High levels of GST-pi are reported in neoplastic cells of mantle cell lymphoma and DLBCL^{44,45} and are correlated with poor prognosis in DLBCL⁴⁴. The role of transcription factor Blimp-1 in PTCL is unclear. We show here that *PRDMI* is expressed at mRNA and protein level in HSTL cells. While inactivation of *PRDMI* through epigenetic mechanisms has been recently reported in NKTCL suggesting a role as tumor suppressor gene^{30,46}, its expression has been associated with chemoresistance in T-cell lymphoma²⁹.

Tumor development is a multistep process involving deregulation of oncogenes and tumor suppressor genes (TSG). To date, no oncogene or TSG has been identified in HSTL. *AIM1* is a gene whose expression is altered in association with tumor suppression in a model of human melanoma²⁸. It is frequently deleted or methylated in several solid tumors and in myeloma and more interestingly NK cell lines^{14,30,31}. Altogether, these data and our findings that *AIM1* is dramatically reduced in HSTL most likely due to promoter methylation suggest that *AIM1* might play a role as a TSG in HSTL oncogenesis and provide rationale for testing demethylating agents

in this disease. Our expression data also suggests that the recurrent iso7q aberration in HSTL could target putative TSG and oncogenes, including *IKZF1* and *PTPN12*.

With respect to potential target for novel therapies in HSTL, we also show here Syk expression by neoplastic HSTL cells with constitutive activation in DERL2 cells compared to normal T cells. Syk is a protein tyrosine kinase involved in B-cell receptor signaling and its activation is associated with cell growth and survival in B-cell lymphomas^{47,48}. Normal mature T lymphocytes lack Syk expression⁴⁹. However, Syk protein has been recently reported as a feature common to most PTCLs, which potentially represents a novel therapeutic target, since, in addition to its aberrant expression in many PTCLs, inhibition of Syk induces apoptosis and blocks proliferation in T-cell lymphoma cell lines^{32,49}. An orally available Syk inhibitor is currently being tested for B-cell lymphomas in a phase I/II clinical trial, with encouraging results⁵⁰. In view of the findings that Syk inhibition induced apoptosis in DERL2 cells in a dose-dependent manner, Syk could also be a potential candidate target for pharmacologic inhibition in HSTL.

In conclusion, we show that the distinctive molecular signature of HSTL partly reflects the ontogeny and might explain several clinicopathologic features of the disease including the homing to sinusoids of the spleen and bone marrow. The study highlights emerging oncogenic pathways, potentially implicated in the pathophysiology of the disease. It may offer rationale for exploring new therapeutic options such as tyrosine kinase inhibitors and demethylating agents in these patients. Finally, this study also provides additional molecular arguments for grouping $\alpha\beta$ and $\gamma\delta$ HSTL as a single distinct entity.

ACKNOWLEDGEMENTS

This work is part of the Carte d'Identité des Tumeurs (CIT) program (<http://cit.ligue-cancer.net/index.php/en>) from the Ligue Nationale Contre le Cancer and of the Tenomic project

supported by a Programme Hospitalier de Recherche Clinique and the Institut National du Cancer (INCa). This work was supported by the Institut National de la Santé et de la Recherche Médicale (INSERM), the Institut National du Cancer (INCa), the Plan cancer of the Belgian government, and the Association pour la Recherche Thérapeutique, Génétique et Immunologique dans les Lymphomes (ARTGIL). M.T. was supported by the Fondation pour la Recherche Médicale (DEQ 2010/0318253). We are extremely thankful for the contributions made by Christelle Thibault from the IGBMC platform (Affymetrix : Philippe Kastner). We also thank Joe A. Trapani for providing antibodies, L. Del Vecchio for providing DERL2 cell line, Francois Radvanyi for critical opinion in data interpretation, Jérôme Cuvillier and Nadine Vailhen from GELAP, and Virginie Fataccioli and Maryse Baia for their technical assistance

Appendix : List of contributors to the TENOMIC project :

A. Martin, Hôpital Avicenne, Bobigny ; I. Soubeyran, P. Soubeyran, Institut Bergonié, Bordeaux ; P. Dechelotte, A. Pilon, Pr O.Tournilhac, Hôtel-Dieu, Clermont Ferrand ; P. Gaulard, MH Delfau, A Plonquet, C. Haïoun, Hôpital H Mondor, Créteil ; T. Petrella, L. Martin, JN Bastié, O Casanovas CHU, Dijon ; B. Fabre, D. Salameire, R. Gressin, D. Leroux, MC Jacob CHU, Grenoble ; L. De Leval, B. Bisig, G. Fillet, C. Bonnet, CHU of Liège ; M.C. Copin, B. Bouchindhomme, F. Morschhauser, CHU, Lille ; B. Petit, A. Jaccard, Hôpital Dupuytren, Limoges, F. Berger, B. Coiffier, CHU Sud, Lyon ; T. Rousset, P. Quittet, G. Cartron, Hôpital Gui de Chauliac-St Eloi, Montpellier ; S. Thiebault, B. Drenou, Hôpital E. Muller, Mulhouse ; K. Montagne, S. Bologna, CHU de Brabois, Nancy ; C. Bossard, S. Le Gouill, Hôtel-Dieu, Nantes ; T. Molina, Hôtel-Dieu, Paris ; J. Brière, C. Gisselbrecht, Hôpital St Louis, Paris ; B. Fabiani, A Aline-Fardin, P. Coppo, Hôpital Saint-Antoine, Paris ; F. Charlotte, J. Gabarre, Hôpital Pitié-Salpêtrière, Paris ; J. Bruneau, D. Canioni, V. Verkarre, E Macintyre, V. Asnafi, O. Hermine, R. Delarue, F Suarez, D. Sibon, JP Jais, Hôpital Necker, Paris ; M. Parrens, JP Merlio, E Laharanne, K. Bouabdallah, Hôpital Haut Lévêque, Bordeaux ; S.Maugendre-Calet, P. Tas, T. Lamy, CHU Pontchaillou, Rennes ; JM Picquenot, F. Jardin, C. Bastard, Centre H Becquerel, Rouen ; M. Peoc'h, J. Cornillon, CHU, Saint Etienne ; L. Lamant, G. Laurent, Lucie Oberic, Hôpital Purpan, Toulouse ; J.Bosq, P. Dartigues, V. Ribrag, Institut G Roussy, Villejuif ; M. Patey, A. Delmer, Hôpital R. Debré, Reims ; JF Emile, K. Jondeau, Hôpital Ambroise Paré, Boulogne ; MC Rousselet, Mathilde Hunault, CHU, Angers ; C. Badoual, Hôpital européen Georges Pompidou, Paris ; C. Legendre, S. Castaigne, AL Taksin, CH Versailles, Le Chesnay ; J. Vadrot, A. Devidas, CH Sud francilien, Corbeil ; Dr Gandhi DAMAJ, CHU Amiens, Hématologie Clinique. F Lemonnier, M Travert, INSERM , Créteil ; P Dessen, G Meurice, Institut G Roussy, Villejuif ; M Delorenzi, E Missiaglia, N Houhou, Swiss Institut of Bioinformatics, Lausanne ; F Radvanyi, E Chapeaublanc, Institut Curie, Paris ; S Spicuglia, CIML, Marseille ; J Soulier, Hôpital St Louis, Paris ; C Thibault, IGBMC, Illkirsch
GELA/GOELAMS

AUTHORSHIP:

Contribution: P.G. L.d.L and M.T. designed research; M.T., Y.H., A.d.R., N.M-G., Ja.B. and T.M. performed research; M.T., A.d.R., and P.G. analyzed and interpreted the data; L.d.L., Ja.B., J.B., B.P., and P.G. collected data; PG and A.d.R. supervised bioinformatics analyses , T.M. contributed vital analytical tools; M.T., A.d.R., L.d.L. and P.G. drafted the manuscript.

Conflict-of-interest disclosure: The authors declare no competing financial interests.

Correspondence: Philippe Gaulard, MD, Département de Pathologie and Inserm U955, Hôpital Henri Mondor, 94010 Créteil, France; e-mail : philippe.gaulard@hmn.aphp.fr.

References

1. Gaulard P, Bourquelot P, Kanavaros P, et al. Expression of the alpha/beta and gamma/delta T-cell receptors in 57 cases of peripheral T-cell lymphomas. Identification of a subset of gamma/delta T-cell lymphomas. *Am J Pathol.* 1990;137:617-628.
2. Farcet JP, Gaulard P, Marolleau JP, et al. Hepatosplenic T-cell lymphoma: sinusal/sinusoidal localization of malignant cells expressing the T-cell receptor gamma delta. *Blood.* 1990;75:2213-2219.
3. Cooke CB, Krenacs L, Stetler-Stevenson M, et al. Hepatosplenic T-cell lymphoma: a distinct clinicopathologic entity of cytotoxic gamma delta T-cell origin. *Blood.* 1996;88:4265-4274.
4. Belhadj K, Reyes F, Farcet JP, et al. Hepatosplenic gammadelta T-cell lymphoma is a rare clinicopathologic entity with poor outcome: report on a series of 21 patients. *Blood.* 2003;102:4261-4269.
5. Mackey AC, Green L, Liang LC, Dinndorf P, Avigan M. Hepatosplenic T cell lymphoma associated with infliximab use in young patients treated for inflammatory bowel disease. *J Pediatr Gastroenterol Nutr.* 2007;44:265-267.
6. Macon WR, Williams ME, Greer JP, Cousar JB. Paracortical nodular T-cell lymphoma. Identification of an unusual variant of peripheral T-cell lymphoma. *Am J Surg Pathol.* 1995;19:297-303.
7. Suarez F, Wlodarska I, Rigal-Huguet F, et al. Hepatosplenic alphabeta T-cell lymphoma: an unusual case with clinical, histologic, and cytogenetic features of gammadelta hepatosplenic T-cell lymphoma. *Am J Surg Pathol.* 2000;24:1027-1032.
8. Swerdlow SH, Campo E, Harris NL, et al. WHO Classification of Tumors of Haematopoietic and Lymphoid Tissues. IARC: Lyon. 2008.
9. Wlodarska I, Martin-Garcia N, Achten R, et al. Fluorescence in situ hybridization study of chromosome 7 aberrations in hepatosplenic T-cell lymphoma: isochromosome 7q as a common abnormality accumulating in forms with features of cytologic progression. *Genes Chromosomes Cancer.* 2002;33:243-251.
10. Bennett M, Matutes E, Gaulard P. Hepatosplenic T cell lymphoma responsive to 2'-deoxycoformycin therapy. *Am J Hematol.* 2010;85:727-729.

11. de Leval L, Rickman DS, Thielen C, et al. The gene expression profile of nodal peripheral T-cell lymphoma demonstrates a molecular link between angioimmunoblastic T-cell lymphoma (AITL) and follicular helper T (TFH) cells. *Blood*. 2007;109:4952-4963.
12. Piccaluga PP, Agostinelli C, Califano A, et al. Gene expression analysis of peripheral T cell lymphoma, unspecified, reveals distinct profiles and new potential therapeutic targets. *J Clin Invest*. 2007;117:823-834.
13. Iqbal J, Weisenburger DD, Chowdhury A, et al. Natural killer cell lymphoma shares strikingly similar molecular features with a group of non-hepatosplenic gammadelta T-cell lymphoma and is highly sensitive to a novel aurora kinase A inhibitor in vitro. *Leukemia*. 2011;25:348-358.
14. Huang Y, de Reynies A, de Leval L, et al. Gene expression profiling identifies emerging oncogenic pathways operating in extranodal NK/T-cell lymphoma, nasal type. *Blood*. 2010;115:1226-1237.
15. Iqbal J, Weisenburger DD, Greiner TC, et al. Molecular signatures to improve diagnosis in peripheral T-cell lymphoma and prognostication in angioimmunoblastic T-cell lymphoma. *Blood*. 2010;115:1026-1036.
16. Ballester B, Ramuz O, Gisselbrecht C, et al. Gene expression profiling identifies molecular subgroups among nodal peripheral T-cell lymphomas. *Oncogene*. 2006;25:1560-1570.
17. Miyazaki K, Yamaguchi M, Imai H, et al. Gene expression profiling of peripheral T-cell lymphoma including gammadelta T-cell lymphoma. *Blood*. 2009;113:1071-1074.
18. Delfau-Larue MH, Dalac S, Lepage E, et al. Prognostic significance of a polymerase chain reaction-detectable dominant T-lymphocyte clone in cutaneous lesions of patients with mycosis fungoides. *Blood*. 1998;92:3376-3380.
19. Kanavaros P, Farcet JP, Gaulard P, et al. Recombinative events of the T cell antigen receptor delta gene in peripheral T cell lymphomas. *J Clin Invest*. 1991;87:666-672.
20. Correia DV, d'Orey F, Cardoso BA, et al. Highly active microbial phosphoantigen induces rapid yet sustained MEK/Erk- and PI-3K/Akt-mediated signal transduction in anti-tumor human gammadelta T-cells. *PLoS One*. 2009;4:e5657.
21. Zhang Y, Ohyashiki JH, Shimizu N, Ohyashiki K. Aberrant expression of NK cell receptors in Epstein-Barr virus-positive gammadelta T-cell lymphoproliferative disorders. *Hematology*. 2010;15:43-47.
22. Di Noto R, Pane F, Camera A, et al. Characterization of two novel cell lines, DERL-2 (CD56+/CD3+/Tcr γ 5+) and DERL-7 (CD56+/CD3-/TCR γ gammadelta-), derived from a single patient with CD56+ non-Hodgkin's lymphoma. *Leukemia*. 2001;15:1641-1649.
23. Compagno M, Lim WK, Grunn A, et al. Mutations of multiple genes cause deregulation of NF-kappaB in diffuse large B-cell lymphoma. *Nature*. 2009;459:717-721.
24. Caron G, Le Gallou S, Lamy T, Tarte K, Fest T. CXCR4 expression functionally discriminates centroblasts versus centrocytes within human germinal center B cells. *J Immunol*. 2009;182:7595-7602.
25. Travert M, Ame-Thomas P, Pangault C, et al. CD40 ligand protects from TRAIL-induced apoptosis in follicular lymphomas through NF-kappaB activation and up-regulation of c-FLIP and Bcl-xL. *J Immunol*. 2008;181:1001-1011.
26. Capietto AH, Martinet L, Fournie JJ. Stimulated gammadelta T cells increase the in vivo efficacy of trastuzumab in HER-2+ breast cancer. *J Immunol*. 2011;187:1031-1038.
27. Jenne CN, Enders A, Rivera R, et al. T-bet-dependent S1P5 expression in NK cells promotes egress from lymph nodes and bone marrow. *J Exp Med*. 2009;206:2469-2481.
28. Ray ME, Su YA, Meltzer PS, Trent JM. Isolation and characterization of genes associated with chromosome-6 mediated tumor suppression in human malignant melanoma. *Oncogene*. 1996;12:2527-2533.

29. Zhao WL, Liu YY, Zhang QL, et al. PRDM1 is involved in chemoresistance of T-cell lymphoma and down-regulated by the proteasome inhibitor. *Blood*. 2008;111:3867-3871.
30. Iqbal J, Kucuk C, Deleeuw RJ, et al. Genomic analyses reveal global functional alterations that promote tumor growth and novel tumor suppressor genes in natural killer-cell malignancies. *Leukemia*. 2009;23:1139-1151.
31. de Carvalho F, Colleoni GW, Almeida MS, Carvalho AL, Vettore AL. TGFbetaR2 aberrant methylation is a potential prognostic marker and therapeutic target in multiple myeloma. *Int J Cancer*. 2009;125:1985-1991.
32. Feldman AL, Sun DX, Law ME, et al. Overexpression of Syk tyrosine kinase in peripheral T-cell lymphomas. *Leukemia*. 2008;22:1139-1143.
33. Krenacs L, Smyth MJ, Bagdi E, et al. The serine protease granzyme M is preferentially expressed in NK-cell, gamma delta T-cell, and intestinal T-cell lymphomas: evidence of origin from lymphocytes involved in innate immunity. *Blood*. 2003;101:3590-3593.
34. Morice WG, Macon WR, Dogan A, Hanson CA, Kurtin PJ. NK-cell-associated receptor expression in hepatosplenic T-cell lymphoma, insights into pathogenesis. *Leukemia*. 2006;20:883-886.
35. Bendelac A, Savage PB, Teyton L. The biology of NKT cells. *Annu Rev Immunol*. 2007;25:297-336.
36. Kelsen J, Dige A, Schwindt H, et al. Infliximab induces clonal expansion of gammadelta-T cells in Crohn's disease: a predictor of lymphoma risk? *PLoS One*. 2011;6:e17890.
37. Pappu R, Schwab SR, Cornelissen I, et al. Promotion of lymphocyte egress into blood and lymph by distinct sources of sphingosine-1-phosphate. *Science*. 2007;316:295-298.
38. Walzer T, Chiosso L, Chaix J, et al. Natural killer cell trafficking in vivo requires a dedicated sphingosine 1-phosphate receptor. *Nat Immunol*. 2007;8:1337-1344.
39. Marie JP. Drug resistance in hematologic malignancies. *Curr Opin Oncol*. 2001;13:463-469.
40. Andreadis C, Gimotty PA, Wahl P, et al. Members of the glutathione and ABC-transporter families are associated with clinical outcome in patients with diffuse large B-cell lymphoma. *Blood*. 2007;109:3409-3416.
41. Wang B, Li XQ, Ma X, Hong X, Lu H, Guo Y. Immunohistochemical expression and clinical significance of P-glycoprotein in previously untreated extranodal NK/T-cell lymphoma, nasal type. *Am J Hematol*. 2008;83:795-799.
42. Michelutti A, Michieli M, Damiani D, et al. Effect of fludarabine and arabinosylcytosine on multidrug resistant cells. *Haematologica*. 1997;82:143-147.
43. Tew KD. Glutathione-associated enzymes in anticancer drug resistance. *Cancer Res*. 1994;54:4313-4320.
44. Ribrag V, Koscielny S, Carpiuc I, et al. Prognostic value of GST-pi expression in diffuse large B-cell lymphomas. *Leukemia*. 2003;17:972-977.
45. Bennaceur-Griscelli A, Bosq J, Koscielny S, et al. High level of glutathione-S-transferase pi expression in mantle cell lymphomas. *Clin Cancer Res*. 2004;10:3029-3034.
46. Kucuk C, Iqbal J, Hu X, et al. PRDM1 is a tumor suppressor gene in natural killer cell malignancies. *Proc Natl Acad Sci U S A*. 2011.
47. Pogue SL, Kurosaki T, Bolen J, Herbst R. B cell antigen receptor-induced activation of Akt promotes B cell survival and is dependent on Syk kinase. *J Immunol*. 2000;165:1300-1306.
48. Gururajan M, Dasu T, Shahidain S, et al. Spleen tyrosine kinase (Syk), a novel target of curcumin, is required for B lymphoma growth. *J Immunol*. 2007;178:111-121.
49. Wilcox RA, Sun DX, Novak A, Dogan A, Ansell SM, Feldman AL. Inhibition of Syk protein tyrosine kinase induces apoptosis and blocks proliferation in T-cell non-Hodgkin's lymphoma cell lines. *Leukemia*. 2010;24:229-232.

50. Friedberg JW, Sharman J, Sweetenham J, et al. Inhibition of Syk with fostamatinib disodium has significant clinical activity in non-Hodgkin lymphoma and chronic lymphocytic leukemia. *Blood*. 2010;115:2578-2585.

Table 1. Summary of clinical, pathological, immunohistochemical, and cytogenetic features of patients enrolled in the study.

EBI ID	Age (at dx)	Sex	Diagnosis	Organ	Type of sample	CD3	CD2	CD5	CD7	CD4	CD8	βF1	δTCR	CD56	TiA1	GzmB	EBV ^o	T clone	Cytogenet
HSTL_02	41	F	HSTL γδ	Spleen	Tissue	+	+	-	-	-	-	-	* +	+	+	-	-	+ R(Jδ) G(β)	iso7q (+)
HSTL_03	73	F	HSTL γδ	Spleen	Tissue	+	+	-	-	-	+	-	+	+	+	+	-	+	iso7q (-)
HSTL_04	38	M	HSTL γδ	Spleen	Tissue	+	nd	-	-	-	-	+	+ **	-	+	-	-	+	iso7q (+) trisomy 8
HSTL_05	56	M	HSTL αβ	Spleen	Tissue	+	nd	-	nd	-	-	+	-	-	-	-	-	+	iso7q (+)
HSTL_06	53	F	HSTL αβ	Spleen	Tissue	+	-	-	+	-	-	+	-	+	+	-	-	+	iso7q (-)
HSTL_08	24	F	HSTL γδ	Blood	Cell suspension (no cell sorting)	+	nd	-	+	-	-	-	+	+	+	nd	nd	+	
HSTL_09	36	M	HSTL γδ	Blood	Cell suspension (cell sorting CD56+) Purity 77%	+	+	-	+	-	-	-	+	+	+	-	nd	+	iso7q (+)
HSTL_01	86	F	HSTL γδ	Spleen	Cell suspension (cell sorting CD3+ CD56+) Purity 84%	+	+	-/+	nd	-	-	-	+	+	+	-	-	+	iso7q (-)
HSTL_10	67	M	HSTL γδ	Spleen	Tissue	+	+	-	+	-	-	-	+ **	-	+	-	-	+	Iso7q (-)
HSTL_07 DERL2	30	M	HSTL γδ	Blood	Cell line	+	+	-	+	-	+		+	+			-		Iso7q (+)

(*) HSTL_02 with a γδ HSTL phenotype at diagnosis disclosed a TCR-silent phenotype (βF1-, δTCR1-) at the time of analysis.

(**) δ chain rearrangement determination using a GC-clamp multiplex polymerase chain reaction (PCR)-δ-DGGE procedure

(^o) EBV investigation by in situ hybridization with EBERs probes and/or immunohistochemistry with LMP-1 antibody

Table 2: Selection of genes differentially expressed in HSTL primary tumors compared to PTCL,NOS with *P*-value less than 0.001. A complete list of genes is given in the supplemental table S1.

Genes overexpressed in HSTL compared to PTCL,NOS

Gene class and specific genes	Fold change
NK cell associated molecules	
KLRC3	73,95
KIR2DS2	33,03
KLRD1	25,39
CD16	11,83
KIR3DL2	21,58
KLRB1	17,52
KIR3DS1	16,88
KIR2DL2	20,35
KIR3DL1	19,85
KIR2DL3	16,35
KIR3DL3	18,95
KIR2DL1	17,42
KLRC4	14,41
NCAM	18,04
CD244	10,65
KIR2DS5	11,59
KIR2DL5A	12,02
KIR2DS1	9,47
KIR2DS3	9,05
KLRG1	9,39
KLRC1 /// KLRC2	10,37
KIR2DL3 /// KIR2DL4 /// KIR2DL5A	6,04
CTSW (Cathepsin w)	6,76
KLRK1	6,45
Microenvironment	
Hemoglobin gamma	17,62
Hemoglobin beta	15,13
Hemoglobin alpha	14,39
DEFA1 /// DEFA1B /// DEFA3	13,64
CCL3 (MIP1)	4,44
Chemokines	
CXCL7 (PPBP)	21,06
CXCL6	8,96
Multi Drug Resistance	
ABCB1 (MDR1)	11,72
ABCB1 /// ABCB4	6,74
Oncogenes	
MYBL1	18,81
VAV3	3,86

Cell adhesion // Cell to cell interaction	
CD11d	48,35
PGM5	6,90
T cell receptor	
TRA@ // TRD@	13,22
TARP // TRGC2	10,94
Transcription factors	
TCF21	12,87
PRDM16	7,86
WT1	3,70
Growth Factors	
IGFBP2	7,52
AREG (amphiregulin)	8,96
PDGFD	7,83
Extracellular matrix interaction	
ADAMTS17	12,93
Others	
S1PR5	49,99

Genes downregulated in HSTL compared to PTCL,NOS

Chemokines	
CCL19	0,011
CXCL9	0,016
CCL18	0,041
CXCL10	0,044
TFH signature	
CXCL13	0,057
CD200	0,165
ICOS	0,158
CXCR5	0,246
Immunomodulation	
IDO1	0,074
IL4I1	0,160
Tumor suppressor	
AIM1	0,195
Others	
TIAM1	0,097
CD5	0,209

Table 3: Selection of genes differentially expressed in HSTL primary tumors compared to NKTCL with *P*-value less than 0.001. A complete list of genes is given in the supplementary table S1.

Genes overexpressed in HSTL compared to NKTCL

Gene class and specific genes	Fold change
NK cell associated molecules	
KLRB1	17,26
KLRG1	6,81
Microenvironment	
Hemoglobin delta	32,87
Hemoglobin alpha	22,79
Hemoglobin beta	19,46
Hemoglobin gamma	15,18
CD36	14,63
T cell receptor	
TARP//TRGC2	11,12
CD3D	7,34
CD3G	6,89
CD247 (CD3Z)	3,82
Chemokines	
CXCL7	23,27
CXCL6	10,73
Transcription factors	
NR4A2	17,77
TCF21	11,72
GATA6	6,16
PRDM16	5,99
PRDM1	2,81
Signal transduction	
SPRY2	9,87
PLCB1	9,66
MAP4K3	7,81
RHOB	7,61
SPRY1	5,59
MAP3K5	2,35
Wnt signaling	
TCF7L2	6,35
TLE1	5,55
Oncogenes	
VAV3	5,25
FYN	4,29
MAF	3,46
Multi Drug Resistance	
ABCB1	2,54
Growth factor	
PDGFD	9,26
Cell adhesion/ extracellular matrix	

CD11d	28,67
ADAMTS17	9,53
Apoptosis	
BCL2L1	4,59
Cell cycle	
CCNL1	3,34
CCND3	2,42
Others	
S1PR5	39,64
TMEM178	32,26
TANC1	32,24
FCRL3	20,27
CD5L	14,89
CXXC5	14,83

Genes downregulated in HSTL compared to NKTCL

Cytotoxic molecules	
Granzyme B	0,15
Granzyme K	0,21
Chemokines	
CXCL10	0,05
Apoptosis	
BIRC5	0,26
Immunomodulation	
IL4I1	0,26
Tumor suppressor	
AIM1	0,26

Table 4 : Selection of genes differentially expressed in HSTL primary tumors compared to normal $\gamma\delta$ T cells with *P*-value less than 0.01. A complete list of genes is given in the supplementary table S1.

Genes overexpressed in HSTL compared to normal $\gamma\delta$ T cells with $p < 0.01$		
Gene class and specific genes	Fold change	
	Activated	Resting
Oncogenes		
FOS *	6,50	
VAV3 °	3,52	3,67
MAF		4,42
NK cell associated molecules		
KIR2DS2 * °	13,98	16,63
KLRC3 * °	11,33	14,87
KIR3DL1//KIR3DL2 * °	9,56	11,16
KIR2DL1 * °	8,90	7,57
KIR2DL2 * °	8,60	8,85
KIR2DS5 * °	7,26	5,19
KIR3DS1 * °	7,03	6,34
KIR2DL3 * °	6,83	9,06
KIR2DL5A * °	6,40	6,09
KIR3DL3 * °	5,75	6,51
KLRC4 * °	5,70	5,17
KIR2DS3 * °	5,69	6,34
KIR2DS1 * °	5,00	5,17
KIR2DS4 * °	3,23	3,67
CD244 *	7,23	3,18
NCAM1 *	6,27	
Microenvironment		
Hemoglobin beta	46,31	34,14
Hemoglobin alpha	34,93	24,06
CXCL12	31,57	27,39
Immunoglobulin	26,29	21,08
CD163	8,86	
Signal transduction		
SPRY2 * °	13,77	33,98
RHOB * °	7,03	
MAP4K3 * °	5,96	9,18
SPRY1 * °	6,50	7,97
Sonic hedgehog		
GLI3 *	8,86	5,94
PRKAR2B *	8,25	3,15
PRKACB °	3,25	3,75
PRKAR1A °	2,80	7,63
Tyrosine kinase		
SYK *	10,59	2,68
Cell adhesion		
CD11d * °	37,57	33,11
VCAM1	15,06	71,58
ICAM1		5,71

Wnt pathways

FRZB	14,01	14,19
TCF7L2 *	10,96	
BAMBI	8,58	7,52
TLE1 *	7,16	4,48
CTNNB1 *	3,99	11,24
APC	3,60	2,33
FZD5	2,53	3,43
Others		
S1PR5 *	8,16	3,51

Genes downregulated in HSTL compared to normal $\gamma\delta$ T cells with $p < 0.01$

Cytotoxic molecules

Granulysin * °	0,03	0,03
Granzyme H * °	0,03	0,05
Granzyme B *	0,04	0,17
Granzyme K * °	0,26	0,10

Chemokines

LTA *	0,02	
TNF	0,03	
IFNG *	0,03	

Tumor suppressor

AIM1 * °	0,34	0,24
----------	------	------

Others

CD5 * °	0,24	0,20
---------	------	------

* genes also differentially expressed in HSTL cells compared to normal activated $\gamma\delta$ T cells.

° genes also differentially expressed in HSTL cells compared to normal resting $\gamma\delta$ T cells.

Table 5: Summary of immunohistochemical results

	HSTL (n=20)	DERL2
FosB	5*/14	-
CD163	0/3	ND
ICAM1	0/7	ND
VCAM1	4°/12	ND
Granzyme H	0/7	-
Beta-catenin	0/5	ND
Syk	8/9	+
Blimp-1	7/7	+
Bcl10	5/5	ND
GSTP1	4/4	ND
CD56	9/17	+

° 2 with weak (equivocal) staining in TC.

* Double immunostaining showing presence of FosB-positive lymphocytes coexpressing CD2 or TIA1 in 3 investigated cases

ND : Not done

Table 6 : Selection of pathways differentially expressed in HSTL compared to PTCL, NOS, NKTCL or normal $\gamma\delta$ T cells.

Pathway name	HSTL vs PTCL,nos	HSTL vs NKTCL	HSTL vs activated $\gamma\delta$ T cell	HSTL vs resting $\gamma\delta$ T cell
	Globaltest P value	Globaltest P value	Globaltest P value	Globaltest P value
Biocarta 133 - Ras-Independent in NK cell-mediated cytotoxicity	3.E-06	3.E-02	3.E-04	3.E-03
KEGG 04650 - Natural killer cell mediated cytotoxicity	5.E-06	7.E-03	7.E-05	3.E-03
KEGG 04370 - VEGF signaling pathway	6.E-06	1.E-03	2.E-04	3.E-03
KEGG 04060 - Cytokine-cytokine receptor interaction	6.E-06	4.E-03	1.E-04	7.E-03
Biocarta 131 - Phospholipase C Signaling Pathway	7.E-06	3.E-04	3.E-03	8.E-02
Biocarta 140 - Selective expression of chemokine receptors during T-cell polarization	7.E-06	3.E-02	5.E-05	1.E-02
Biocarta 506 - Sprouty regulation of tyrosine kinase signals	8.E-06	2.E-04	2.E-04	3.E-03
KEGG 04310 - Wnt signaling pathway	1.E-05	7.E-04	2.E-04	3.E-03
Biocarta 590 - Sonic Hedgehog (Shh) Pathway	1.E-05	5.E-03	6.E-05	3.E-03
Biocarta 137 - Regulation of BAD phosphorylation	1.E-05	7.E-03	9.E-05	3.E-03
KEGG 04010 - MAPK signaling pathway	1.E-05	3.E-03	2.E-04	3.E-03
KEGG 04340 - Hedgehog signaling pathway	3.E-05	1.E-03	5.E-04	2.E-02
Biocarta 586 - Multi-Drug Resistance Factors	1.E-05	5.E-03	2.E-02	Ns
Biocarta 465 - Role of MEF2D in T-cell Apoptosis	3.E-05	1.E-03	6.E-04	3.E-03
KEGG 04660 - T cell receptor signaling pathway	3.E-05	3.E-03	8.E-05	Ns
KEGG 04630 - Jak-STAT signaling pathway	4.E-05	9.E-03	1.E-04	3.E-03
KEGG 04620 - Toll-like receptor signaling pathway	5.E-05	7.E-03	5.E-04	7.E-03
KEGG 04514 - Cell adhesion molecules (CAMs)	6.E-05	3.E-03	3.E-04	7.E-03
KEGG 04210 - Apoptosis	7.E-05	1.E-02	1.E-04	3.E-03
KEGG 04150 - mTOR signaling pathway	1.E-04	3.E-03	2.E-04	3.E-03
KEGG 04330 - Notch signaling pathway	2.E-04	1.E-03	3.E-04	2.E-02
KEGG 04670 - Leukocyte transendothelial migration	3.E-04	1.E-02	1.E-03	3.E-03
KEGG 05200 - Pathways in cancer	3.E-04	2.E-02	5.E-04	3.E-03
KEGG 04110 - Cell cycle	1.E-02	5.E-03	3.E-03	3.E-03
KEGG 03050 - Proteasome	5.E-03	3.E-03	2.E-04	1.E-02

FIGURE LEGENDS

Figure 1: HSTL samples cluster separately to the other T-cell lymphomas, irrespective of their $\alpha\beta$ or $\gamma\delta$ T-cell lineage

Unsupervised consensus clustering of gene expression profiles of 9 HSTL, 7 NKTCL, 16 PTCL,NOS and 17 AITL tumor samples. Core clusters (C1, C2, C3, C4) are defined as groups of at least 5 samples being co-clustered in at least 14 of the 16 initial partitions (see M&M), and are individualized by the horizontal red line. Fisher exact test p-values for association between the consensus partition C1/C2/C3/C4 and sample's annotations (Lymphoma.type, Material.type, TCR.type) are shown in red.

Lymphoma.type : {H : Hepatosplenic T-cell lymphoma (HSTL); N : NK/T-cell lymphoma, nasal type (NKTCL); A : Angioimmunoblastic T-cell Lymphoma (AITL); P : Peripheral T-cell lymphoma, not otherwise specified (PCTL,NOS)}

Material.type { C: cell line; S : sorted tumor cells; T : tissue sample }

TCR.type : T-cell Receptor type { A: alpha-beta ; G: gamma-delta}(NA: not available)

Figure 2: Validation of selected genes by quantitative RT-PCR analysis.

qRT-PCR analysis for *S1PR5*, *ABCBI*, *FOS*, *FOSB*, *RHOB*, *VAV3* and *KIR3DS1* in HSTL tissues (n=10), cells (n=3), PTCL,NOS (n=14) and NKTCL (n=6). The results are expressed as relative fold change compared with normal $\gamma\delta$ T cells sorted from spleen. Values for each sample were normalized to *GAPDH*. Arbitrary value of 1 was assigned to normal $\gamma\delta$ T cells.

Figure 3: Validation of genes overexpressed in gene expression profiling by immunohistochemistry.

Representative HSTL disclosed staining of neoplastic cells for (A) FOSB, (B) SYK, (C) CD56, (D) BCL10, (E) GSTP1 and (F-G) PRDM1. Panel G refer to DERL2 cells. Staining of NK cells

for (H) Granzyme H were observed. Images were captured with a Zeiss Axioskop2 microscope (Zeiss). Photographs were taken with an Olympus DP70 camera. Images were acquired with Olympus DP Controller 2002, and images were processed with Adobe Photoshop Version 7.0 (Adobe Systems). Original magnification, $\times 400$ (A-L).

Figure 4: Cellular programs deregulated in HSTL: * correspond to resting $\gamma\delta$ T cells.

Representative molecular pathways, among those differentially expressed (as shown by enrichment analysis, see tables 6 and S5) in HSTL by comparison with NKTCL, PTCL,NOS and normal $\gamma\delta$ T cells, are illustrated (A: Natural killer-cell mediated cytotoxicity; B: T-cell receptor signaling pathway; C: Sprouty regulation of tyrosine kinase signal pathway; D: Sonic hedgehog pathway; E: Multi-drug resistance factors and F: Cell cycle). For each line, green corresponds to the minimal intensity value (min), red corresponds to the maximal intensity value (max), and black corresponds to $(-\max - \min)/2$.

Figure 5: *AIM1* is methylated in HSTL DERL2 cell line

(A) Real-time PCR quantification of *AIM1* was evaluated in normal $\gamma\delta$ T cells, HSTL tissues, HSTL cells, DERL2 cells, PTCL,NOS and NKTCL. The results are expressed as relative fold change compared with normal $\gamma\delta$ T cells sorted from spleen. Each sample was normalized to *GAPDH*. (B) Localization of CpG islands (CpG1 and CpG2) in the *AIM1* promoter and schematic representation of the sequenced genomic fragments including all CpG sites (vertical bars). Approximate spacing of the CpG dinucleotides is shown for the 44 CpGs of island 1 and the 119 CpGs of island 2 (Top). Ten representative clones from DERL2 cells are presented, only 43 CpGs of island 2 were represented because of unmethylation of the first 76 CpGs (Left). Example of methylated cytosines after bisulfite-converted genomic DNA treatment (Right). Methylated CpG, ●; Unmethylated CpG, ○.

(C) Real-time PCR quantification of *AIM1* was evaluated in DERL2 cells after 96 hours of 10 μ M or 40 μ M decitabine treatment (every 24hours) with or without 500nM TSA treatment for the last 24 hours. (D) DERL2 cell line were cultured with or without 10 μ M or 40 μ M of decitabine for 96 hours (decitabine was added every 24 hours). Cellular apoptosis was analyzed using 7AAD staining.

Figure 6: SYK a potential candidate target for pharmacologic inhibition

(A) Histogram representation of affymetrix datas of overexpressed *SYK* probe set in HSTL tissues, HSTL cells, normal $\gamma\delta$ T cells and DERL2 cells. (B) Immunostaining of SYK in DERL2 cell line. (C) Western blot analysis of Syk, phosphorylated Syk tyr525/526 and loading control beta actin. (D) DERL2 cell line or normal activated $\gamma\delta$ T cells were cultured with 40 μ M or 60 μ M of Syk inhibitor II or vehicle alone for 48 hours. Apoptosis was analyzed using 7AAD staining. For normal activated $\gamma\delta$ T cells, TCRV γ 9 apoptotic cells were determined by measuring the pourcentage of TCRV γ 9+ 7AAD+ cells. * correspond to p<0.05.

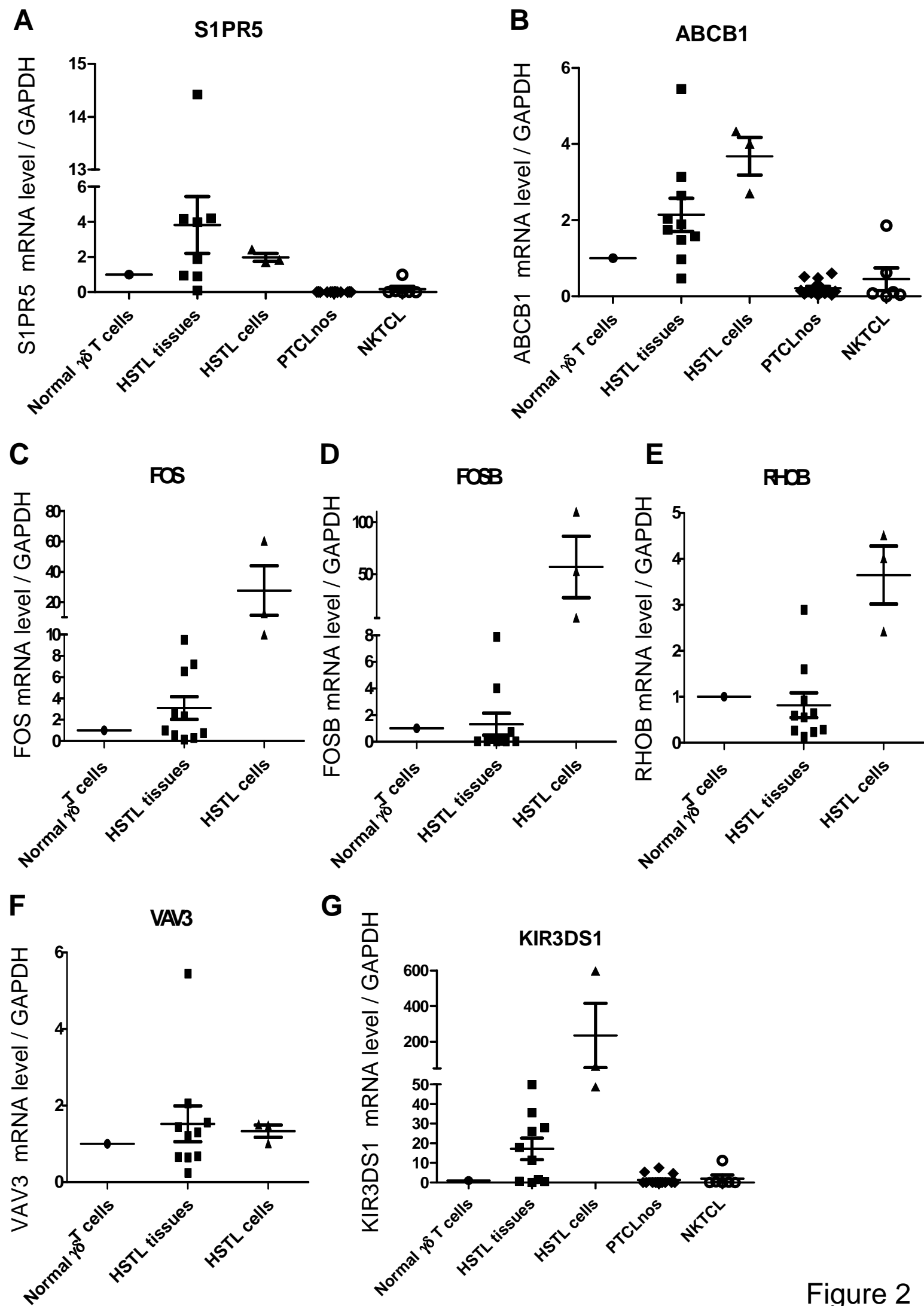


Figure 2

Figure 3

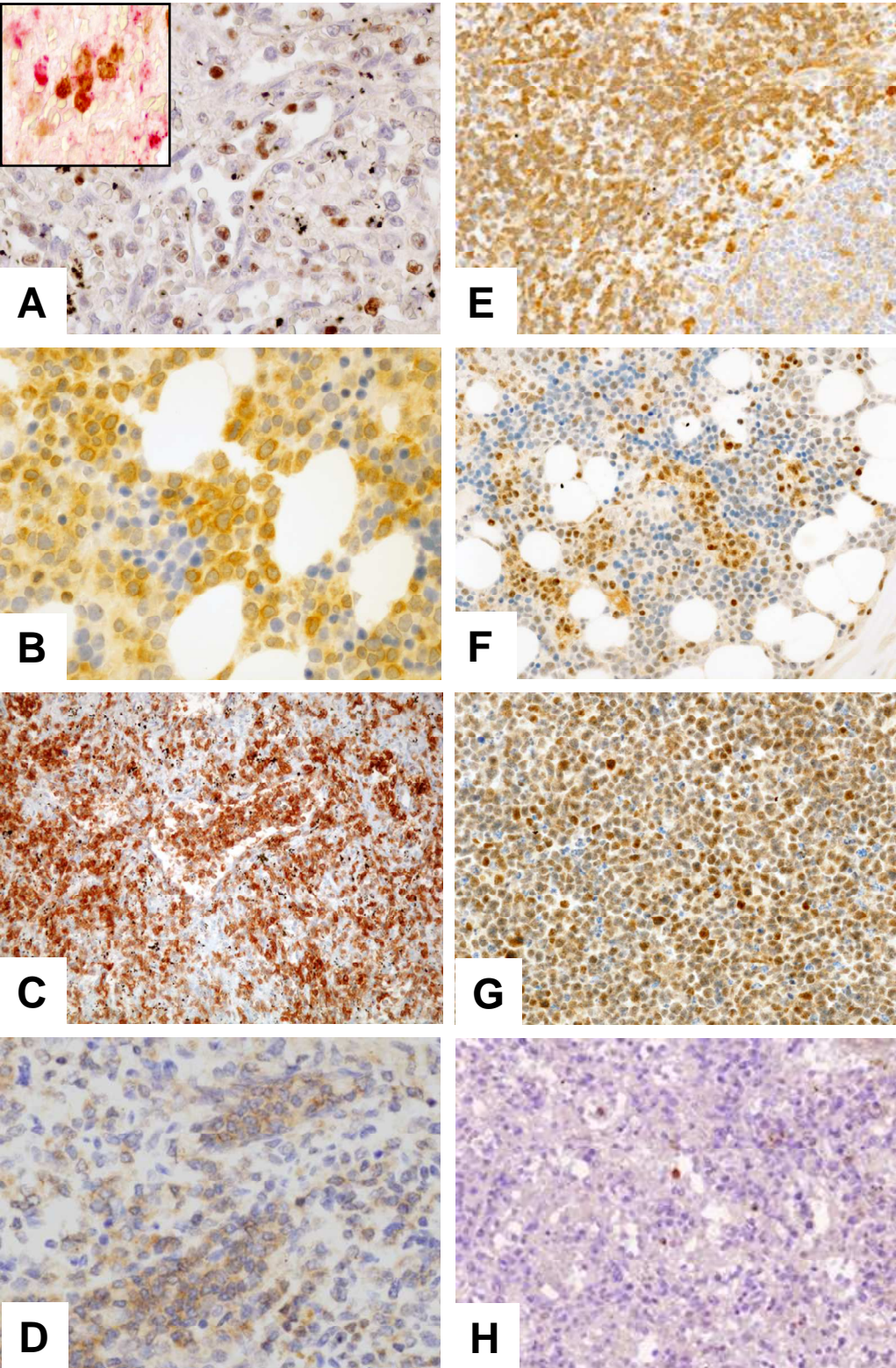


Figure 4

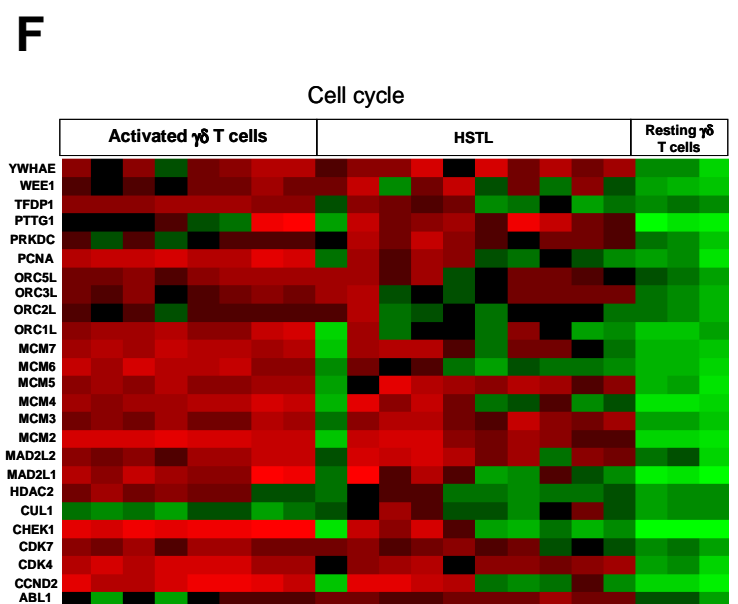
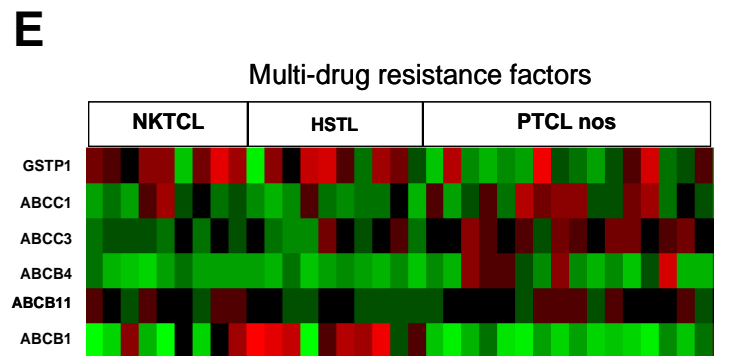
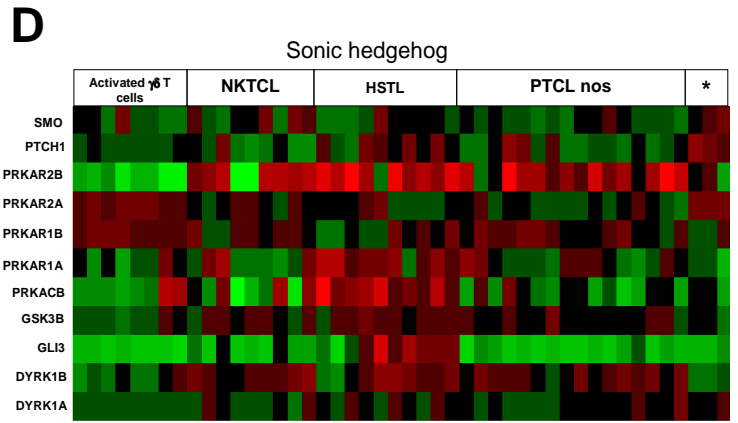
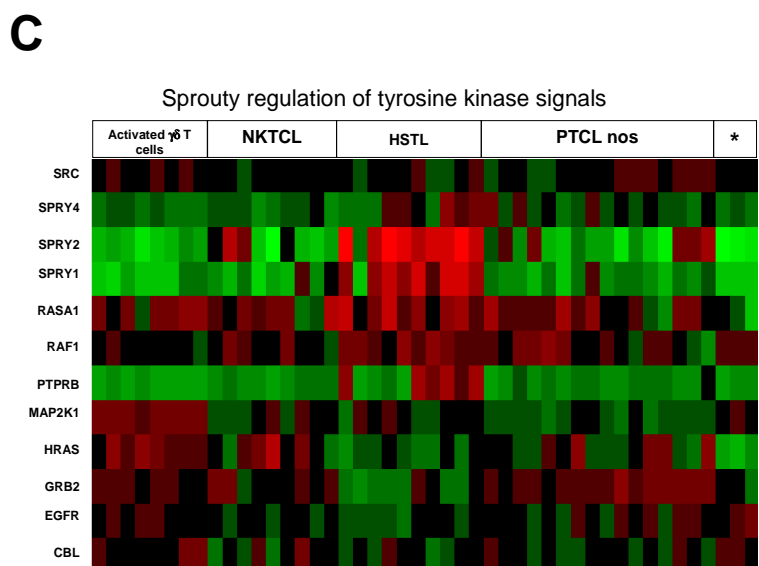
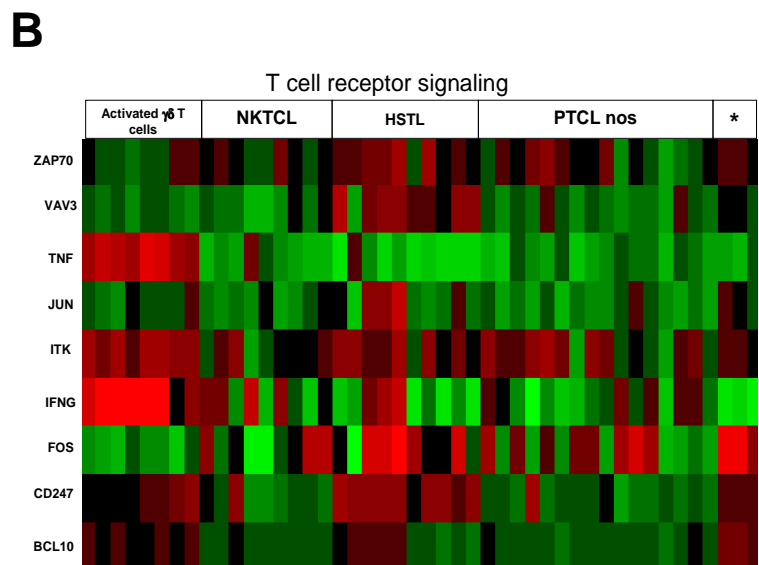
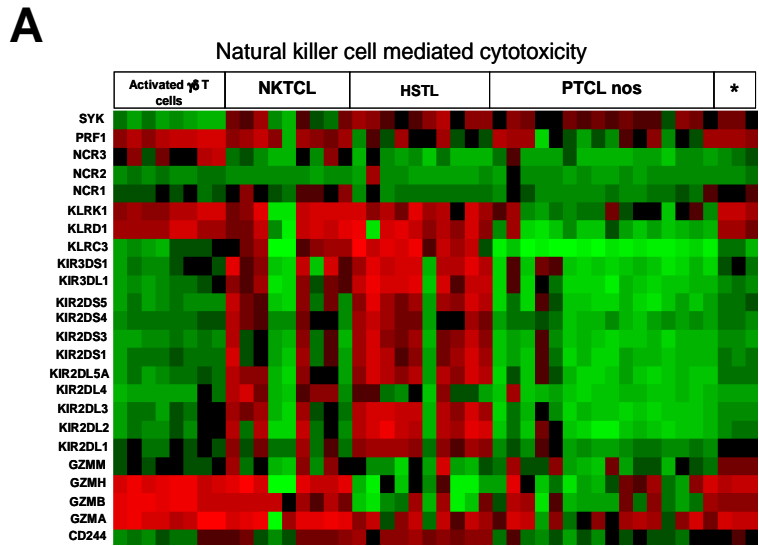
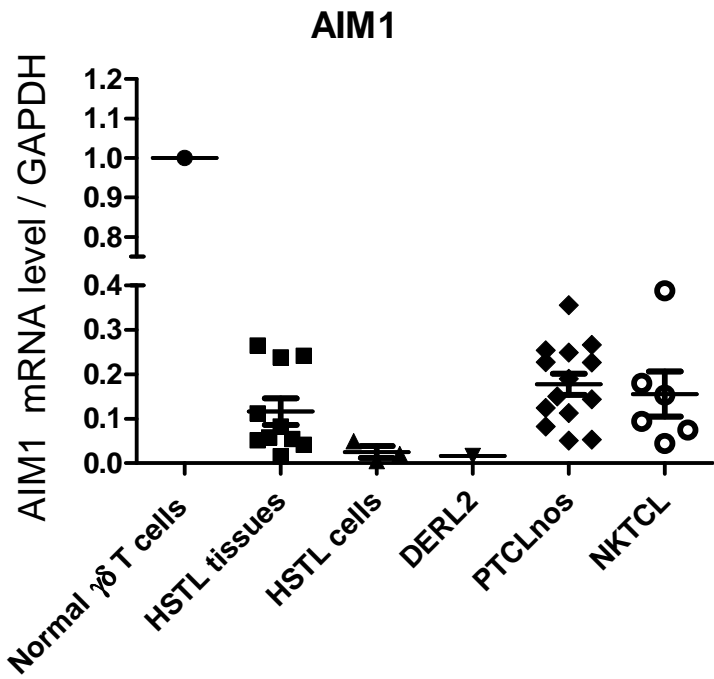
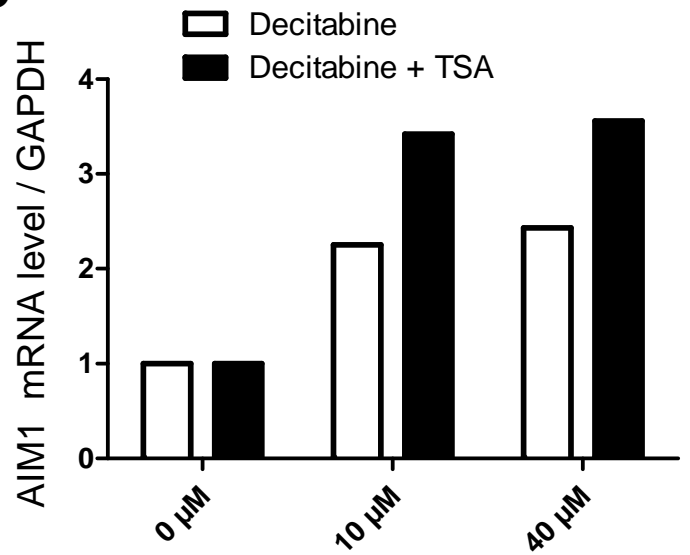


Figure 5

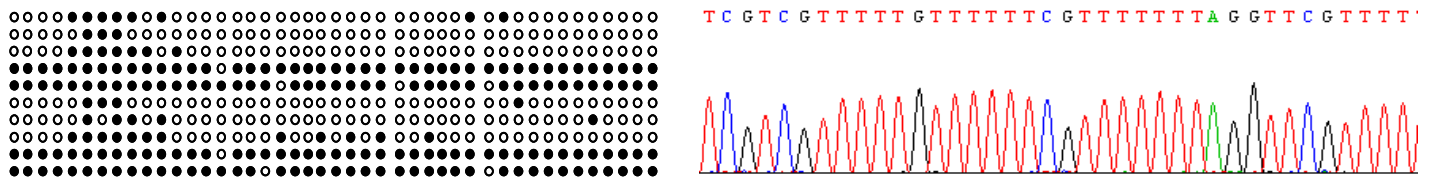
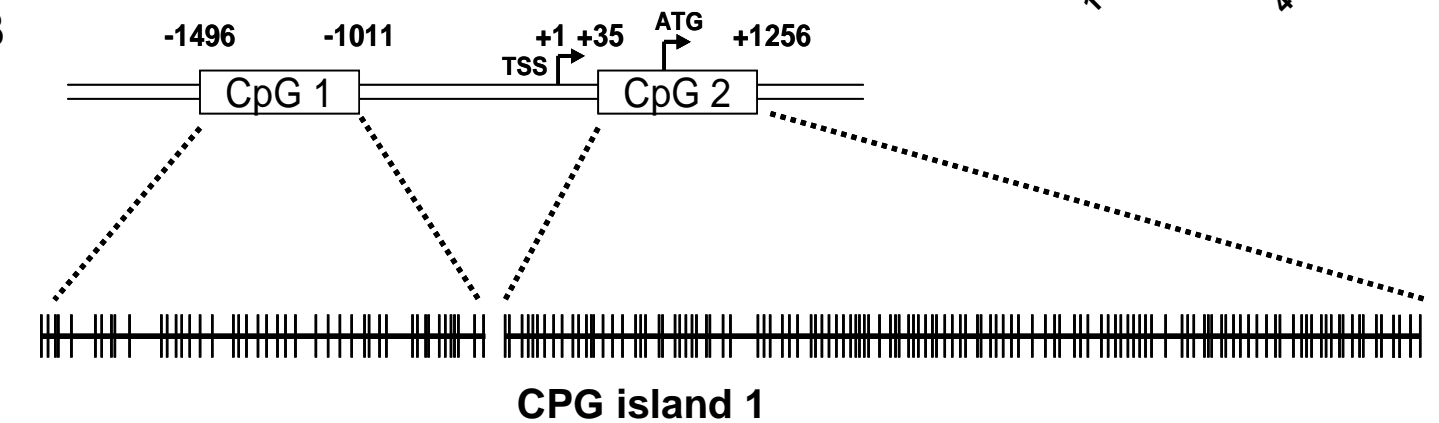
A



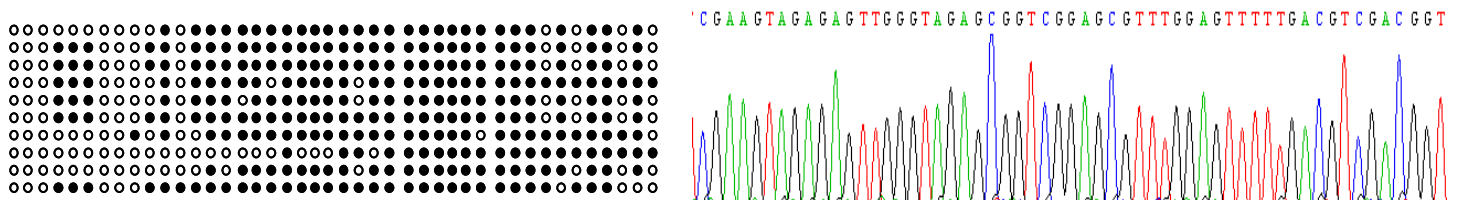
C



B



CPG island 2



D

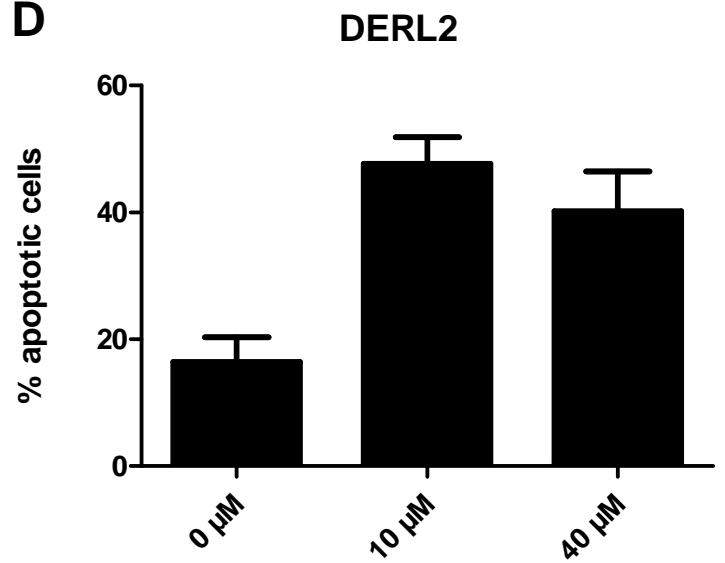


Figure 6

